HIGH RESOLUTION SEAMLESS MAPPING OF CHANG'E-5 LANDING AREA USING LROC NAC IMAGES. K. Di, M. Jia, X. Xin, B. Liu, Z. Liu, M. Peng, Z. Yue, State Key Laboratory of Remote Sensing Science, Institute of Remote Sensing and Digital Earth, Chinese Academy of Sciences, Beijing 100101, China. (dikc@radi.ac.cn)

Introduction: Chang'e-5, China's first sample return mission, will be launched in 2019, and the planned landing area is near Mons Rümker in Oceanus Procellarum [1, 2]. Landing area mapping is of great importance for supporting scientific analysis and safe landing. Among the orbital images acquired by different lunar missions, Lunar Reconnaissance Orbiter Camera (LROC) narrow angle camera (NAC) images have the highest spatial resolution of up to 0.5m [3], which can reveal detailed surface features such as small craters and large rocks that may not be discernible in other images and mapping products. Tens of LROC NAC controlled mosaics have been produced by LROC team and made available on the the LROC PDS archive webpage as of 2014 [4]. Recently, the Lunar North Pole Mosaic (LNPM) of 60-90 °N has been produced and made available at lroc.sese.asu.edu/gigapan [5]. It is necessary and valuable to produce high resolution NAC mosaic of the planned landing area of Chang'e-5 mission.

In this research, we have developed a systematic method and procedure to produce seamless digital orthophoto map (DOM) of Chang'e-5 landing area using over 700 LROC NAC images. The resultant seamless DOM coves a large area (20° longitude × 4° latitude) and is tied to SLDEM 2015, which is a widely used reference DEM produced by co-registration and combining SELENE TC DEM with LRO laser altimetric (LOLA) data [6]. The regional context of Chang'e-5 landing area is shown in Fig.1.

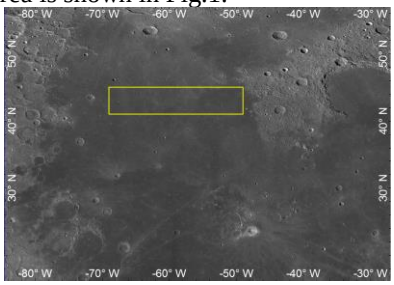

Fig. 1. Planned landing area of Chang'e-5, marked as rectangle on LROC WAC mosaic.

Data: The Chang'e-5 landing area covers a large area of 443.7km × 121.4km. As of December 2017, there are 2299 NAC images within or overlapping with this area and can be downloaded from the LROC website (http://lroc.sese.asu.edu). We select 765 images for the mapping task, they are generally of good quality, similar solar azimuth angles, and similar resolutions (0.5~2m). SLDEM2015 is downloaded from the PDS LOLA data node (http://imbrium.mit.edu/EXTRAS/SLDEM2015/), and is used as reference for geopositioning and DOM generation. LROC wide angle camera (WAC) global mosaic is downloaded from LROC web site [7] and is used as a bridge for matching between NAC images and SLDEM2015.

Methodology: The method we developed for large area seamless mapping consists of two stages of data processing: stage 1 includes local block adjustment with rational function model (RFM) and seamless local DOM generation; stage 2 includes whole area adjustment of the local DOMs with thin plate spline (TPS) model and seamless DOM mosaicking.

In stage 1, the whole area is divided into 11 blocks, each covering an area of (3° longitude × 4° latitude) and having sufficient overlaps. The rigorous sensor models (RSMs) of all the NAC images are established using collinearity equations with interior and exterior orientation elements retrieved from the corresponding SPICE kernels. The RFM, which can approximate RSM with a precision of 1/100 pixel level in image space, is used to replace RSM without loss of accuracy in the subsequent processing [8, 9]. Rational polynomial coefficients (RPCs) of each image are derived by least-squares fitting using vast numbers of virtual control points generated by the RSM. In order to reduce the inconsistencies among the neighboring LROC images, local block adjustment is performed for each block based on RFM+Affine model, that is, instead of re-computation of RPCs for each image in the block, Affine transformation parameters are solved in a least squares manner for each image so that to refine the RFM model of the image. For the local block adjustment, tie points are extracted by image matching among NAC images; control points are extracted by matching between NAC images and the WAC mosaic using image correlation technique, and the planimetric and vertical coordinates are obtained from the well co-registered LROC WAC mosaic and SLDEM2015 respectively. After the local block adjustment, seamless DOMs of the 11 blocks are generated using the refined RFMs and SLDEM2015. The resultant DOMs are of high internal precision and have been tied to SLDEM2015. As can be seen in Fig. 2, the inconsistencies between neighboring NAC images have been effectively removed after the block adjustment. Due to the precision limitation of the control points, some in-

consistencies between the neighboring blocks still exist. In addition to geometric adjustment, radiometric correction is also applied through histogram matching using the WAC mosaic as a reference.

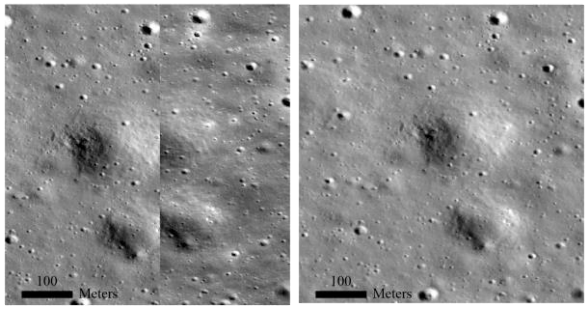

Fig. 2. Comparison of the seams between DOMs of neighboring images before (left) and after (right) block adjustment.

In stage 2, a TPS model is applied to all the blocks in order to remove the inconsistencies between the neighboring block DOMs. Constrained by control points, TPS can tackle non-rigid deformations effectively[10, 11]. In this research, control points for TPS are extracted by image matching in the overlapping areas between the neighboring block DOMs. We choose the block DOM which has the best positioning accuracy in the first stage as a reference. In addition, to avoid over-correction in the non-overlapping areas, we define virtual control points in the borders of the whole area and keep their coordinates unchanged in this stage. After the TPS based correction, the non-rigid inconsistencies among the block DOMs are effectively removed and a whole area seamless DOM is produced through mosaicking.

Results: The precision of the local block adjustments is evaluated using the root mean square (RMS) errors of residuals at the tie points and control points. As a result, the RMS errors of the tie points of all the 11 blocks in image space are all around half pixel, with the minimum of 0.37 pixel and the maximum of 0.58 pixel, indicating a satisfactory precision. The RMS errors of the control points of all blocks are around 20 pixels, equivalent to half the size of SLDEM2015 grid cell, indicating that the local DOMs are tied to SLDEM2015 well. Figure 3 is a zooming-out display of the resultant seamless DOM mosaic of Chang'e-5 landing area with a spatial resolution of 1.5 m and image size of 224721 columns × 44945 rows. Since radiometric corrections haven been made in stage 1 and there are sufficient overlaps among the blocks, the whole area DOM mosaic is not only geometrically seamless, but also radiometrically homogeneous.

Conclusions: We developed a two-stage adjustment method for large area seamless lunar mapping, which can reduce the inconsistencies among the neighboring LROC NAC images and tie the images to SLDEM2015. Based on the method, a high resolution seamless DOM has been generated in the planned landing area of Chang'e-5 mission using 765 LROC NAC images. The DOM is valuable for detailed morphological study of the landing area. The developed method can be applied to produce high-resolution seamless DOMs using LROC NAC images for other interested large areas of the moon surface.

Acknowledgment: This work was supported by the National Natural Science Foundation of China (Grant Nos. 41671458, 41590851, 41771490).

References: [1] Xinhuanet. (2017) http://news.xinhuanet.com/2017-06/07/c_1121102466.htm. [2] Gbtimes. (2017) https://gbtimes.com/china-confirms-landing-site-change-5-moon-sample-return [3] Robinson, M. S. et al. (2010) *Space Sci. Rev.*, 2010, 150(1), 81-124. [4] Klem, S. M. (2014) *45th LPSC*, abstract # 2885. [5] Wagner, R. V. et al. (2016) *47th LPSC*, abstract # 1582. [6] Barker, M. K. et al. (2016) *Icarus*, 273, 346-355. [7] ASU. (2011) http://wms.lroc.asu.edu/lroc/view_rdr/WAC_GLOBAL. [8] Di, et al. (2003) *PE&RS*, 69, 33-41. [9] Liu, B. et al. (2016) *Int. Archives of Photogrammetry, Remote Sensing and Spatial Information Sciences*, XLI-B4, 441-448. [10] Shen, H. et al. (2013) *Appl. Math. Inform. Sci.*, 7, 555-562. [11] Shen, X. et al. (2017) *ISPRS J. P&RS*, 125, 125–131.

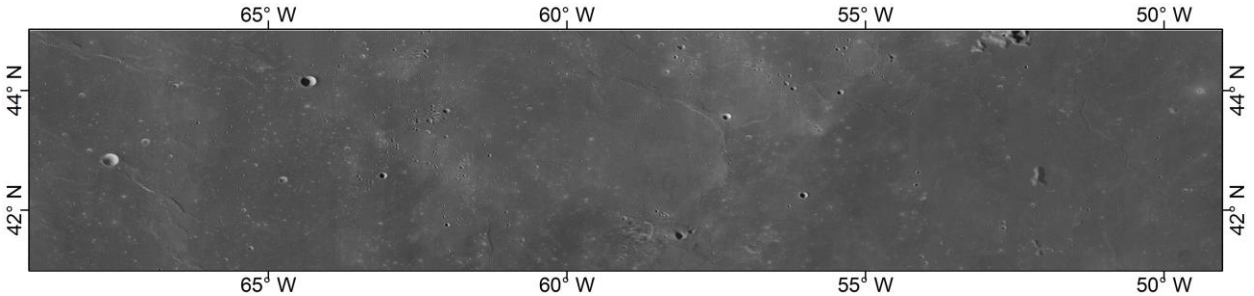

Fig. 3. Zooming-out view of the resultant seamless DOM mosaic of Chang'e-5 landing area.